Non-carbon greenhouse gas emissions for hybrid electric vehicles: three-way catalyst nitrous oxide and ammonia trade-off

Brinklow, G.; Herreros, J. M.; Zeraati rezaei, S.; Doustdar, O.; Tsolakis, A.; Kolpin, A.; Millington, P.

[Link to publication on Research at Birmingham portal](#)

ORIGINAL PAPER

Non-carbon greenhouse gas emissions for hybrid electric vehicles: three-way catalyst nitrous oxide and ammonia trade-off

G. Brinklow[1] · J. M. Herreros[1] · S. Zeraati Rezaei[1] · O. Doustdar[1] · A. Tsolakis[1] · A. Kolpin[2] · P. Millington[2]

Abstract
Transport sector decarbonisation is leading to increased demand for electrified powertrains including hybrid vehicles. The presence of an internal combustion engine and electric motor offer multiple performance and efficiency advantages. However, changes in the conditions that catalytic aftertreatment systems are subjected to can present challenges in meeting forthcoming emissions standards. This work investigated the three-way catalyst performance to abate regulated and unregulated emissions from a gasoline direct injection engine working under conditions related to hybrid vehicle operation. The focus on unregulated emissions of NH_3 and N_2O is of interest due to limited literature on their formation in conventional, and particularly hybrid, vehicle aftertreatment systems. Furthermore, the likelihood of their regulation when the EURO 7 emissions standards are introduced increases the pertinence of this work. For this particular engine and aftertreatment setup, it was found that starting the engine whilst the three-way catalyst temperature was below 150 ℃ led to an increase in tailpipe regulated emissions and N_2O. Whilst, starting the engine when three-way catalyst temperatures were above 350 ℃ lead to tailpipe NH_3 emissions. This was due to the selectivity of NO to form N_2O at lower temperatures and NH_3 at higher temperatures. For the case of the studied catalyst, a vehicle energy management strategy opting to start the engine with the three-way catalyst within a targeted temperature range allowed for a trade-off between regulated emissions, N_2O and NH_3. These findings are significant since it can be used to optimise hybrid vehicle control strategies minimising both regulated and unregulated emissions.

Keywords Catalyst thermal behaviour · Electrified powertrain · EURO 7 · Gasoline aftertreatment · Pollutant emissions · Unregulated emissions

Introduction

The transportation sector contributes up to a third of all anthropogenic CO_2 emissions (The Society of Motor Manufacturers and Traders 2019). In order to tackle this, CO_2 limits in road transport are becoming increasingly stringent worldwide and the EU aims to reduce emissions from 2021 levels by 15% in 2025 to 37.5% in 2030 (International Council on Clean Transportation 2019). To achieve such aggressive targets, vehicle fleets will need to incorporate increased numbers of alternatively fuelled and propelled vehicles. The plug-in hybrid electric vehicle (PHEV), as a medium-term road transport option, has the potential to provide the CO_2 reductions required whilst not compromising on practicality (Orecchini et al. 2018). A PHEV utilises a battery, electric motors and an internal combustion engine (ICE). This means that the ICE will operate differently when compared to ICEs in conventional vehicles. This presents new challenges and opportunities for the operation of the aftertreatment system.

The aftertreatment system of a gasoline direct injection (GDI) engine makes use of a three-way catalyst (TWC)—so-called for its ability to simultaneously convert emissions of CO, NO_X and HC into CO_2, N_2 and H_2O. The performance of a TWC depends significantly upon its temperature. When the TWC is below the light-off temperature (250 ℃–300 ℃)

✉ G. Brinklow
g.brinklow@bham.ac.uk

[1] Department of Mechanical Engineering, School of Engineering, University of Birmingham, Edgbaston, Birmingham B15 2TT, UK

[2] Johnson Matthey Technology Centre, Blount's Court, Sonning Common, Reading RG4 9NH, UK

there is reduced catalyst activity (Fernández-García et al. 2004). When there are multiple engine starts over a single journey—typical of PHEV operation—this problem is exacerbated due to the cooling of the aftertreatment system whilst the engine is off. Therefore, understanding how the TWC operates within the modern set up of a PHEV and improving TWC performance under start-up engine conditions will be vital in order to reduce future harmful emissions and meet future emissions regulations. Furthermore, it is looking increasingly likely that currently unregulated non-carbon species such as ammonia (NH_3) and nitrous oxide (N_2O) will become regulated with the introduction of the EURO 7 emissions regulations. Farren et al. reported that in the UK, the total amount of NH_3 emitted from passenger cars within urban areas was 17 times higher than what had been previously reported by the UK National Atmospheric Emissions Inventory suggesting that NH_3 emissions could be of greater concern then first realised (Farren et al. 2020). However, there has been very little published research into the emissions of NH_3 and N_2O from GDI engines with TWCs during conventional operation and even less so in hybrid vehicles.

NH_3 is a secondary pollutant which is typically formed within the TWC through reactions including NO, CO, H_2O and H_2 as precursor molecules (Heeb et al. 2006; Wang et al. 2019; Liu et al. 2021a, b). The scarce literature agrees on the presence of tailpipe (post-TWC) NH_3 spikes during vehicle accelerations (Heeb et al. 2006; Suarez-Bertoa et al. 2014; Wang et al. 2019; Liu et al. 2021a, b) due to a reduction in engine lambda promoting TWC selectivity towards NH_3 formation (Heeb et al. 2006). Wang et al. (Wang et al. 2019) stated that with catalyst ageing there is a further increase in the selectivity towards NH_3 production. Catalyst temperature has been identified as a key parameter influencing NH_3 formation. A wide temperature range between 250 ℃ and 550 ℃ has been reported where NH_3 selectivity is the highest (Wang et al. 2019). N_2O is also a secondary pollutant formed within the TWC requiring NO as a precursor (Mejía-Centeno and Fuentes 2009). N_2O formation also varies depending upon temperature with different species contributing at different temperatures (Mejía-Centeno and Fuentes 2009). The maximum formation of N_2O was reported to occur between 200 ℃ and 350 ℃ with the principal precursors being CO and NO. Nevalainen et al. acknowledged the reaction between CO and NO, but also stated the role of H_2 and HCs as important N_2O precursor species (Nevalainen et al. 2018).

The start/stop nature of engine operation within PHEVs is likely to increase the frequency and duration of the TWC's operation through the temperature regions where NH_3 and N_2O selectivity is high in comparison with a conventional ICE vehicle. The scarce number of studies that do report unregulated emissions of hybrid electric vehicles (HEVs)

commonly take a holistic approach without investigating the performance of the TWC under such conditions. Suarez-Bertoa et al. reported regulated and NH_3 emissions that were measured from a range extender hybrid vehicle over the WLTC, finding the NH_3 emissions to be comparable to a conventional gasoline vehicle (Suarez-Bertoa 2016). Clarotte et al. also found tailpipe N_2O emissions for light duty hybrid vehicles to be comparable and in some cases even higher than those of conventional gasoline vehicles (Clarotte et al. 2020). The catalyst light-off period has been identified as the source of NH_3 production from HEVs (Suarez-Bertoa et al. 2014; Suarez-Bertoa 2016).

Therefore, a research gap has been identified in the reviewed literature concluding that there is very little available information on the operation of a TWC in an HEV powertrain with respect to currently unregulated non-carbon emissions. This research aims to tackle this gap by investigating the emissions of NH_3 and N_2O over an engine start procedure at multiple TWC temperatures. This is done to replicate the TWC conditions witnessed within a modern hybrid powertrain. NH_3 and N_2O are of interest since it is expected that these will both be regulated with the introduction of the EURO 7 emissions standard (ACEA 2020). The research was undertaken at The University of Birmingham Future Fuels and Powertrains Laboratory.

Materials and methods

Experimental setup

This work was carried out experimentally using a modern turbocharged GDI engine that also featured port fuel injection (details in Table 1). An electric dynamometer was used to control engine speed and load. The testing setup was instrumented to measure appropriate temperatures, pressures and flow rates. The model TWC was provided by Johnson Matthey PLC. The total PGM loading was 30 g/ft³ with 23 g/ft³ of palladium and 7 g/ft³ of rhodium. The

Table 1 Test engine specification

Parameter	Value
Type	Gasoline, port and direct injection
Displacement	1.5 l
Number of cylinders	3
Bore	84 mm
Stroke	90 mm
Compression ratio	11:1
Max. torque	270 Nm
Max. power	133 kW @ 6000 rpm

monolith dimensions were a length of 109 mm and a diameter of 118.4 mm with a cell density of 600/2 and a single layer washcoat loading of 3.0 g/in^3. The monolith was positioned after the turbocharger as shown in Fig. 1. The zoomed in section of the figure labelled 'TWC set up' shows how the TWC was placed with the locations to measure emissions and temperatures before and after the TWC monolith.

Temperature measurements were taken before and after the TWC monolith, using k-type thermocouples and a Pico Technology TC-08 data logger. Two thermocouples were placed before the monolith—one measuring the gas temperature and one measuring the monolith wall temperature on the inlet and outlet faces of the catalyst monolith. A further two thermocouples were placed after the monolith measuring the gas and monolith wall temperatures. Emission probes were located before and after the TWC monolith. Real-time hydrogen emissions were measured using a HSense V&F electron impact ionisation mass spectrometer. All other
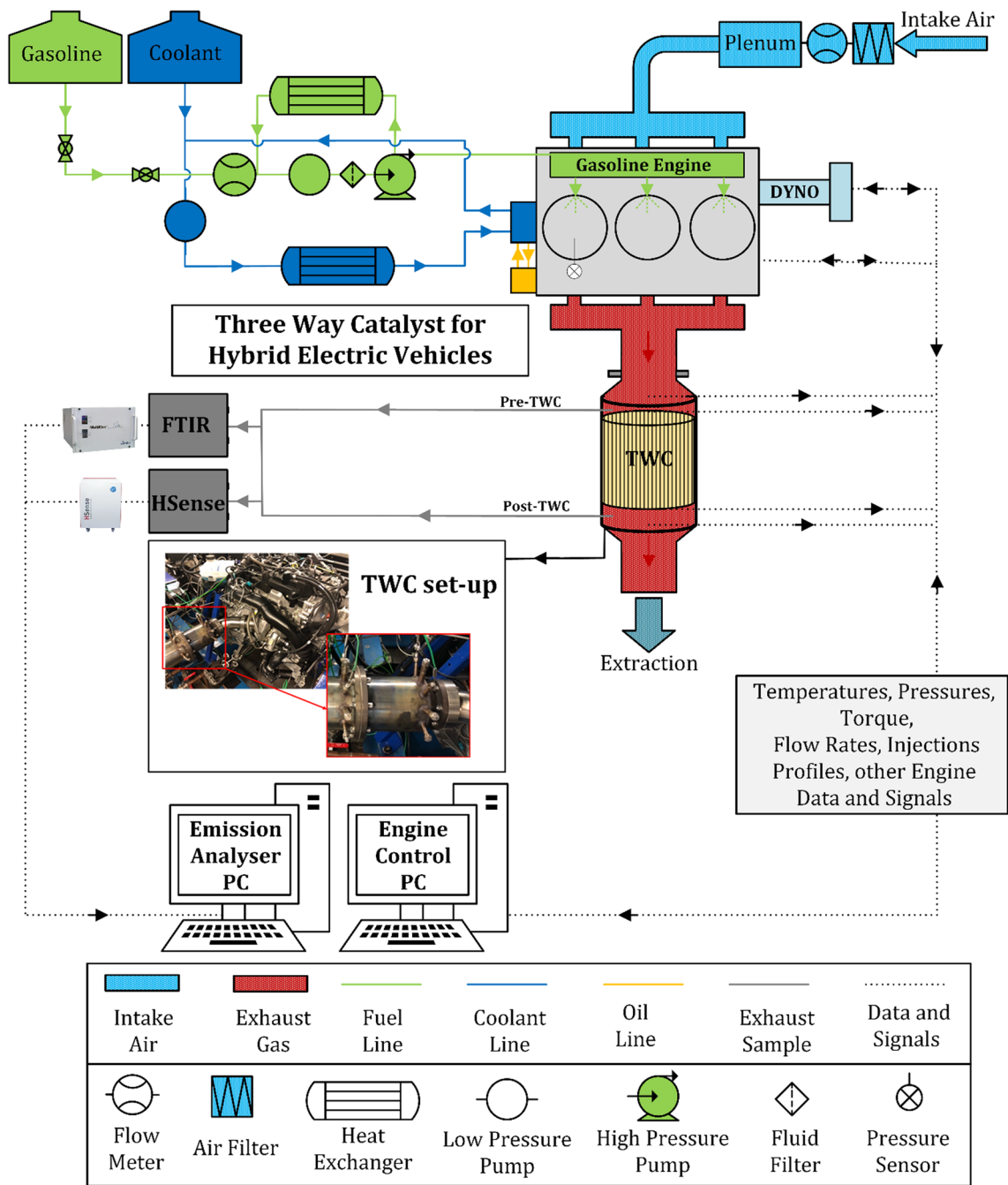

Fig. 1 Engine and TWC setup including locations for emission probes and thermocouples

gaseous emission species, including CO, CO_2, NO_X, NH_3, N_2O and HCs were measured using an MKS multi-gas Fourier transform infrared (FTIR) spectrometer (MKS MultiGAS 2030 Series). Samples were collected as shown in Fig. 1 with heated lines to the analysers. The heated lines were maintained at 150 ℃ to prevent condensation of the water and hydrocarbon species.

Methodology

The engine start procedure was selected in terms of torque and speed. This featured a warmup period of the engine followed by changing to an engine condition with a sufficient power output to charge the battery whilst also operating at a high efficiency point of 2500 rpm and 90 Nm. The engine start cycle completed for each experiment is shown in Fig. 2a. In order to understand how the TWC performs at a variety of conditions the engine was started at various TWC monolith temperatures with three repeats for each temperature. This was achieved by running the engine to heat the TWC before switching the engine off and allowing the TWC to cool to the desired temperature before starting the engine. The monolith temperature at the inlet face was

the temperature that was targeted. To heat the TWC, the engine was operated at 2500 rpm and 90 Nm until the oil, coolant and monolith temperatures had stabilised. Once the temperatures had stabilised the engine was brought to an idle condition of 900 rpm and 3 Nm for 60 s after which the engine was turned off to allow the TWC monolith to cool to the desired temperature. During this period, the engine would also cool with the aim of this to study also how the engine out emissions performance was affected. The cooling of both the catalyst and the engine was desirable as this provided a more realistic comparison to a complete PHEV.

Multiple engine and monolith starting temperatures were selected to cover a wide range of conditions the TWC would be subjected to depending upon the engine off time in a PHEV. The engine starts were chosen to provide TWC monolith start temperatures of ambient, 100 ℃, 150 ℃, 200 ℃, 250 ℃ and 350 ℃. These TWC temperatures were selected based upon previous studies (Zeng et al. 2018; Guille des Buttes et al. 2020) that evaluated a HEV throughout a WLTC and reported TWC temperature. There were multiple engine starts reported by the studies within the range of TWC temperatures selected for our study, particularly during the first part of the WLTC. Temperatures above 350 ℃ were not

Fig. 2 **a** Engine start procedure torque in Nm (solid line) and speed in rpm (dashed line) and **b** exhaust gas flow rate
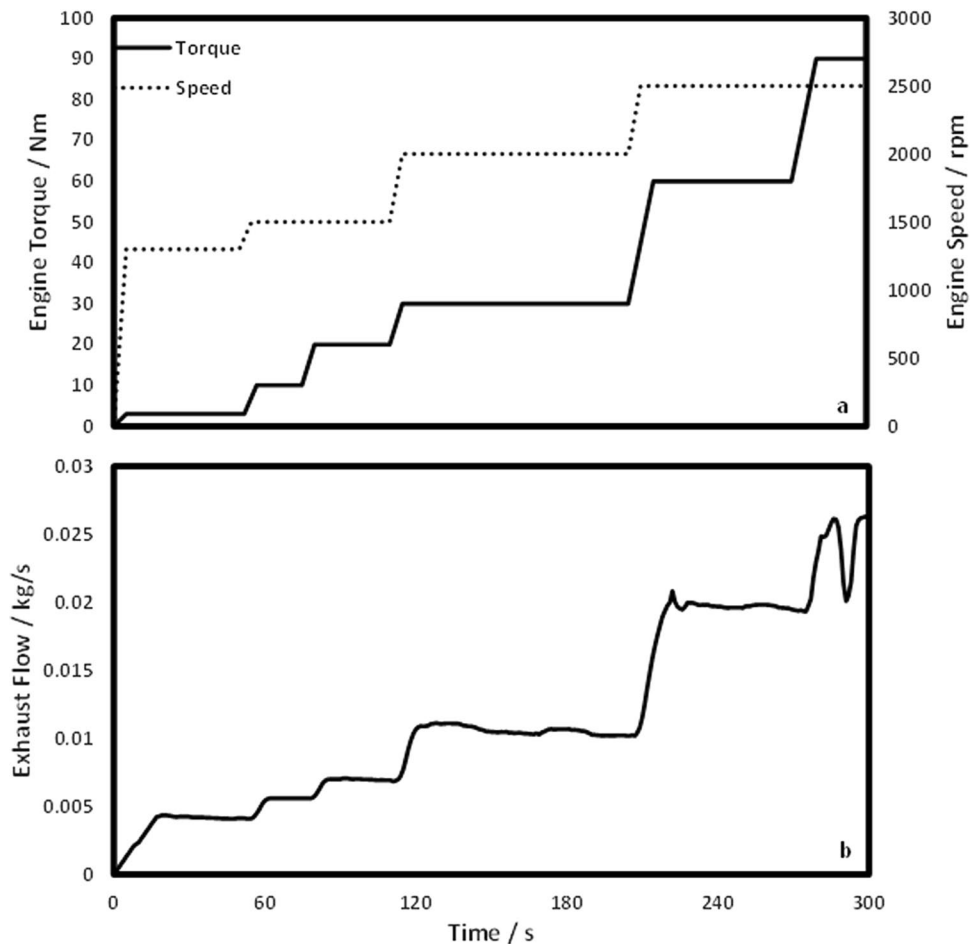
selected, as the TWC will be operated at maximum efficiency. Overall, these testing conditions allowed for study of TWC performance under different pre-TWC emissions and catalyst temperatures both induced from starting the engine at various oil and coolant temperatures. It is considered that the conditions selected are likely to occur within a variety of HEV powertrain architectures (e.g. series, parallel and power-split hybrid), vehicle energy management strategies, and vehicle mode of operation (e.g. charge sustaining and charge depleting). The exhaust gas flow rate was also monitored due to the transient warm up nature of the engine start cycle. This is shown in Fig. 2b as this will also affect TWC performance and total mass of emissions.

The starting TWC, engine oil and coolant temperatures for each of the three repeats are shown in Table 2. This shows how the TWC temperature was linked to the engine start temperature as the engine off period allowed for cooling of not only the TWC but also the engine too. Once the target catalyst temperature was reached the engine started and followed the engine start procedure in Fig. 2 starting with the temperatures shown in Table 2.

Results and discussion

Engine output regulated emissions and TWC conversion performance

The TWC was exposed to different inlet concentrations of pollutants and temperatures depending upon the starting temperature of the engine. Regulated engine output emissions (pre-TWC) for each temperature (average of the three repetitions) are shown in Fig. 3 Since these are the emissions before the TWC these are affected only by the engine temperature. These have been reported as the conditions the TWC is exposed to under HEV operation is of interest in understanding how TWC performance is affected.

The most notable influence that the engine start temperature has on the pre-TWC concentrations is the peak in the CO concentration during the first 10 s of the engine start procedure. This is shown in the zoomed in section of Fig. 3a. There is not an appreciable reduction in the magnitude of

the CO peak until the engine is started with an oil and coolant temperature of 67.2 °C and 67.1 °C, respectively (the 250 °C test—data in Table 2). After this initial peak in CO during the first 10–15 s, the levels of engine out (pre-TWC) CO recorded were similar for each engine start at each temperature. There was increased CO over the first 50 s for the ambient start test, but other than this the levels of CO are comparable. The reason for the larger peaks over the first 50 s in pre-TWC CO emissions for the ambient start was the colder temperatures. Starting the engine at higher temperatures improves the mixture formation in the cylinder minimising CO formation (Bielaczyc et al. 2011). In addition to this, at lower engine start temperatures, the engine runs with a richer fuel mixture in order to improve combustion stability. This will also lead to increased CO emissions (Hu et al. 2007). To minimise the demand on the oxidative capacity of the TWC during the engine start, targeting oil and coolant temperatures of 67.2 °C and 67.1 °C, respectively, should be done. This is because engine temperatures lower than this generates considerably higher concentrations in CO for the TWC to deal with.

The pre-TWC NO_X emissions are plotted in Fig. 3b for each test temperature. By comparing Figs. 2a and 3b, it is clear that the NO_x emissions are affected more so by the engine condition than the other pollutants are. This explains the low concentrations of NO_X during the first 60 s when the engine is idling. Each increase in NO_X concentration matches with an increase in engine load. This is because as the load increases, so too does the in-cylinder temperature resulting in increased NO_X formation via the Zeldovich mechanism (Anetor et al. 2014). The starting temperature of the engine also affects the NO_X concentration that the TWC must deal with. Over the first 150 s, the NO_X emissions are lower when starting the engine with an oil and coolant temperature less than 49.2 °C and 46.4 °C, respectively (results for the ambient and 100 °C tests). This is due to the richer combustion at colder temperatures discussed above and the lower in-cylinder temperatures over the engine start. By keeping the engine load low, it is possible to keep the engine NO_X emissions at or close to zero. Operating at low loads during the engine start could prevent NO_X concentrations being present pre-TWC giving the catalyst time to warm up

Table 2 TWC, oil and coolant temperatures for each engine start

Test	TWC temperature/°C			Oil temperature/°C			Coolant temperature/°C		
	1	2	3	1	2	3	1	2	3
Amb	17.7	17.7	21.2	17.7	16.2	19.6	17.6	16.3	19.6
100 °C	99.6	100.5	100.1	48.5	46.0	50.7	47.0	44.0	47.1
150 °C	150.4	150.2	150.0	57.5	53.3	56.1	56.7	51.2	55.1
200 °C	199.1	199.2	199.2	64.1	59.1	65.0	62.7	58.4	64.4
250 °C	247.7	248.2	249.7	70.1	64.2	70.9	70.3	63.9	71.7
350 °C	350.8	348.2	348.9	83.9	75.7	84.8	81.6	76.3	83.7

Fig. 3 Pre-TWC concentrations for **a** CO, **b** NO_X and **c** THC
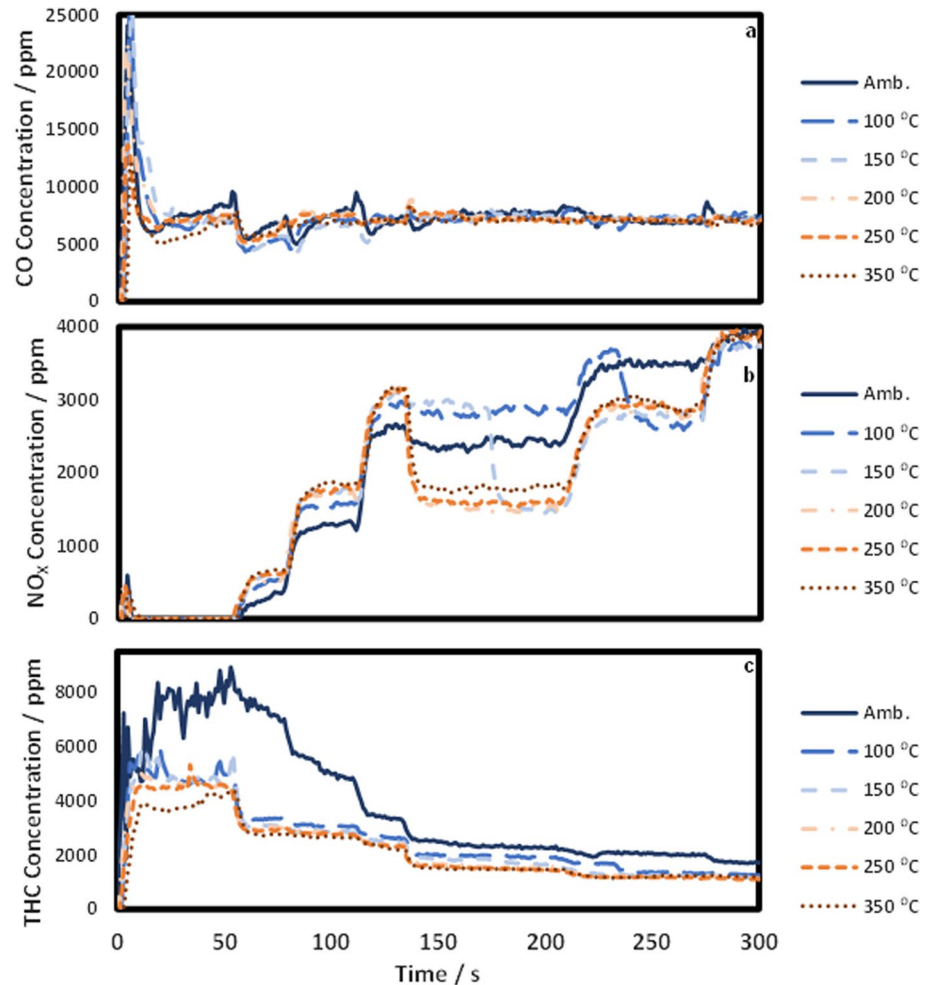
before load is increased. The pre-TWC concentrations of THCs are shown in Fig. 3c. The THCs are the most sensitive to the engine starting temperature with the concentration of THC still higher for the ambient start test even after 300 s. During the 100 s, the concentration of THCs is approximately double for the ambient test (starting oil and coolant temperatures of 18.4 °C) than for the other starting temperatures. This is a result of poorer mixture formation at these low temperatures as well as richer combustion leading to unburnt or partially burnt hydrocarbons (Li and Liu 2011). Even by starting the engine at oil and coolant temperatures of 49.2 °C and 46.4 °C, respectively, provides a considerable reduction in the pre-TWC concentration of THCs and will reduce the demand on the catalyst. There are smaller reductions in the pre-TWC THC concentration at higher start temperatures. It is unlikely that the engine in a PHEV will have to do an ambient start more than once per journey. This is because engine off periods in a PHEV rarely exceed 5 min. When reviewing the literature considering engine performance within a PHEV over different drive cycles, engine off periods varied between 1–5 min (Overington and

Rajakaruna 2015; García et al. 2019; Zhao et al. 2020; Gezer et al. 2021). The time recorded for the engine to cool sufficiently to start the 100 °C experiment was 63 min. Whilst the cooling rate of oil and coolant may be quicker for an engine within a vehicle than those observed in these engine dyno tests due to outside colder temperatures and forced convective cooling as the vehicle continues to travel it is still unlikely that the oil and coolant temperatures will reach such a low level. These conditions though could occur after the vehicle has been left between journeys. The reason why this work opted to use TWC temperature instead of engine off time as the independent variable was to produce results more applicable to different set ups and conditions.

The CO concentration post-TWC (tailpipe) for each of the different start temperature tests is shown in Fig. 4a. The large peaks in CO over the first 10–15 s are still present but now only for the lower catalyst start temperatures (< 150 °C). This is because the catalyst activity when starting at 200 °C or higher is sufficient to oxidise all the CO that is shown in Fig. 3a. Starting the engine with a TWC temperature of 200 °C or greater removes all CO from the exhaust gas. With the
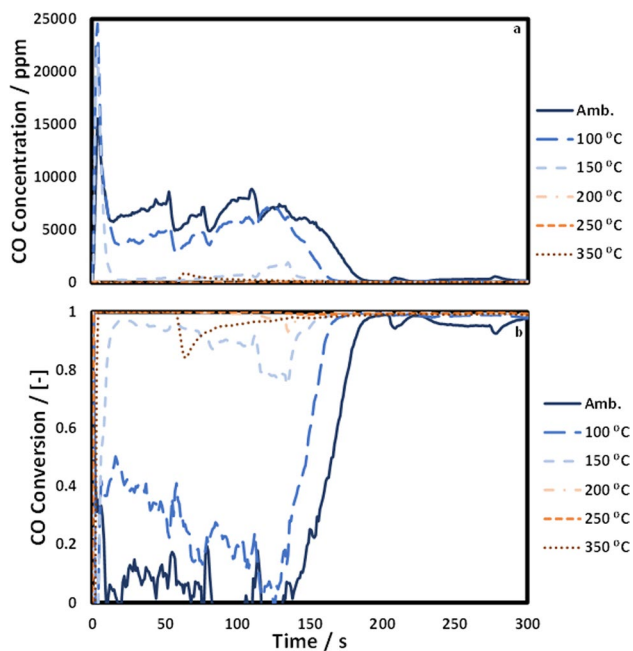
Fig. 4 **a** Post-TWC CO concentration and **b** TWC CO conversion efficiency

Fig. 5 **a** Post-TWC NO$_X$ concentration and **b** TWC NO$_X$ conversion efficiency

exception of the first peak in pre-TWC CO concentration, the inlet concentrations to the TWC were all similar for each test. This highlights that the CO concentrations measured post-TWC are resulting from the reduced TWC performance. This is also shown in Fig. 4b where the conversion efficiency of the TWC is plotted for each test temperature. Starting from a lower temperature not only increases tailpipe CO concentration through increased CO formation in the engine but also through reduced TWC activity. The light-off temperature is defined as the temperature at which 50% conversion is achieved. Using this definition, light-off for CO is achieved immediately for TWC temperatures starting at 200 ℃ or higher. Light-off is reached within the first 10 s for the 150 ℃ experiment, whilst light-off is not reached until 145 s and 165 s for the 100 ℃ and ambient tests, respectively. Whilst there is little change in the light-off time from ambient to 100 ℃, the reduction in light-off time from 100 ℃ to 150 ℃ is substantial. Keeping the TWC temperature at 200 ℃ or above would provide complete CO conversion. However, if this is not possible, a target of 150 ℃ should be set since after this CO conversion deteriorates considerably.

The NO$_X$ concentration post-TWC (engine out) for each of the different catalyst starting temperatures is shown in Fig. 5a. There is little to no NO$_X$ reported post-TWC during the first 60 s of engine operation. This is due to the lack of NO$_X$ pre-TWC (Fig. 3b). After 60 s, when the engine load is increased as per the start-up strategy shown in Fig. 2a, there is a breakthrough in NO$_X$ post-TWC when starting the engine with a TWC temperature at 200 ℃ or lower. On
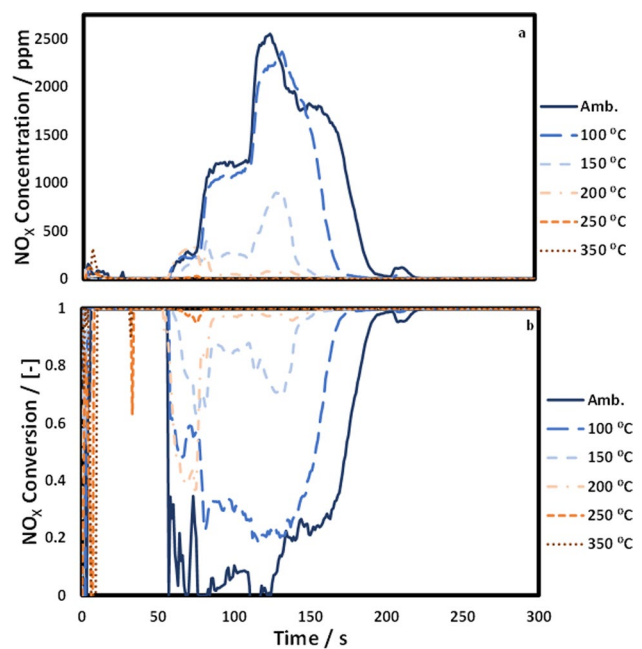
the other hand, starting the engine with a TWC temperature of 250 ℃ or higher completely removes NO$_X$ concentration post-TWC. The NO$_X$ concentration post-TWC follows the same trend as the concentration pre-TWC as each load increase yields an increase in NO$_X$. The conversion efficiency of NO$_X$ is plotted for each of the different starting temperature tests in Fig. 5b. The performance of the TWC can be analysed here by comparing the time taken to reach light-off (50% conversion) once NO$_X$ emissions are present pre-TWC (after 60 s). Light-off is achieved for the ambient test after 174 s and after 154 s for the 100 ℃ test. However, the test starting with a catalyst temperature of 150 ℃ does not drop below 50% conversion. As per the results for CO conversion, there is little improvement when comparing an ambient start to one with a TWC temperature of 100 ℃, but when comparing 100 ℃ to 150 ℃ there is a considerable difference. This could once again be a secondary target if keeping the starting catalyst temperature above 250 ℃ (no NO$_X$) cannot be achieved. A further consideration from these results is the ability to minimise NO$_X$ by operating at a low load condition until the TWC has reached sufficient temperature. Further catalyst heating strategies could be employed such as retarded ignition to help increase catalyst temperature whilst NO$_X$ emissions are kept low. Once the catalyst has reached a sufficient temperature, the engine can then proceed to higher loads and any subsequent NO$_X$ emissions can be converted by the now active TWC. However, this will need to be balanced with the effect on other emissions, fuel economy and driveability.
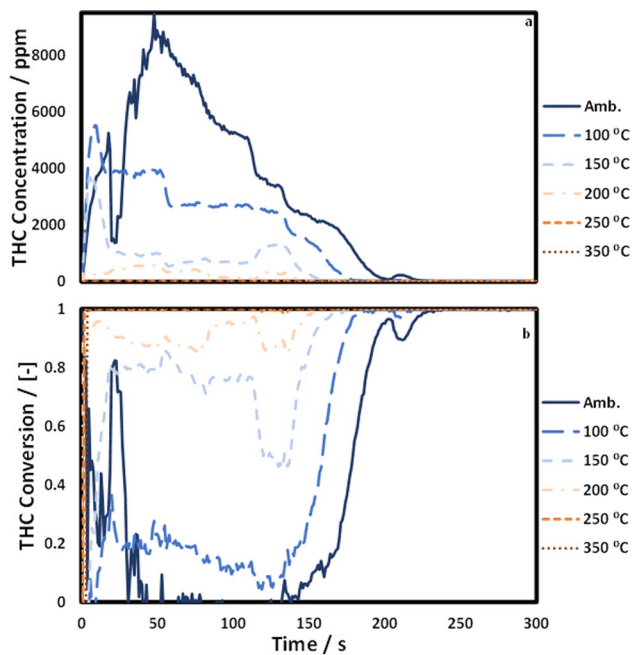
Fig. 6 a Post-TWC THC concentration and **b** TWC THC conversion efficiency

The THC concentration post-TWC for each starting temperature test is shown in Fig. 6a. When starting the engine with a TWC temperature of 250 ℃ or higher there is no THC concentration measured post-TWC. Therefore, total conversion of the THCs pre-TWC (Fig. 3c) is occurring within the TWC. There are low levels of THCs recorded post-TWC for the 200 ℃ catalyst start temperature test. However, for each temperature lower than this the concentrations increase as the temperature is reduced. There is a large difference between the 150 ℃ to the 100 ℃ tests and another large difference between the 100 ℃ and ambient tests. When comparing the different regulated emissions post-catalyst in Figs. 4, 5 and 6, HC species are the most demanding to remove within the TWC. This matched other results in the literature where the $T_{50\%}$ for THC is reported to be higher than that for CO regardless of TWC composition and higher than NO_X for the majority of TWC compositions (Rood, et al. 2020). In the results presented here, HCs require the highest starting catalyst temperature to ensure there is no slip during the engine start. The HC conversion efficiency for each starting catalyst temperature is presented in Fig. 6b. HC conversion takes the longest time out of the regulated pollutants to consistently reach > 90% for the same starting TWC temperature. Light-off was reached after 179 s for the ambient start, after 159 s for the 100 ℃ start and 138 s after the 150 ℃ start. For 200 ℃ and above the conversion efficiency does not fall below 50%. When comparing the performance of the TWC between the 100 ℃ and 150 ℃ starting temperatures there is a large difference before the light-off.

The 100 ℃ starting temperature is at roughly 20% conversion whilst the 150 ℃ starting temperature is at roughly 80% conversion. This same magnitude in conversion efficiency increase was not witnessed for any of the other catalyst start temperatures. Therefore, aiming to start the engine with a monolith temperature greater than 150 ℃ will avoid the substantial drop off in TWC performance witnessed at 100 ℃ when compared to 150 ℃. When starting the engine with a monolith temperature of 250 ℃ or above, there is complete THC conversion. To maintain TWC performance within a HEV experiencing multiple engine starts it would be desirable to keep the monolith temperature at 250 ℃ or above with a second aim of not letting it drop below 150 ℃ if maintaining 250 ℃ is not possible.

Impact of exhaust gas composition and temperature on secondary pollutant formation in TWCs

The formation of NH_3 and N_2O over the TWC has been reported by several studies (Behrentz et al. 2004; Adhikari and Fernando 2006; Anderson et al. 2012; Balas et al. 2014; Badshah and Khalek 2015; Bai et al. 2018; Wang et al. 2019; Awad et al. 2020; Bagheri et al. 2021). The results presented here find agreement with the literature. Whilst there were very little N_2O or NH_3 emissions recorded pre-TWC (< 20 ppm), there were considerable levels of NH_3 and N_2O recorded post-TWC over the first 300 s after the engine had started. These are shown in Fig. 7a, respectively.
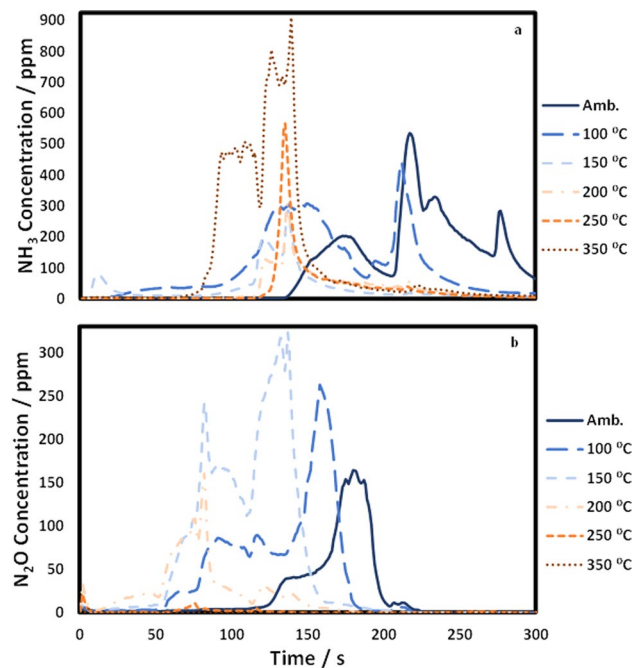

Fig. 7 a Post-TWC concentration of NH_3 and **b** post-TWC concentration of N_2O

Table 3 Cumulative mass emissions for NH_3 and N_2O recorded over the first 500 s of the engine start for each catalyst starting temperature test. The ± figures show the 95% confidence interval calculated from 3 repeats of the start-up test

TWC start temperature/℃	Cumulative mass NH_3/g	Cumulative mass N_2O/g
Amb	0.329 ± 0.015	0.009 ± 0.008
100	0.172 ± 0.029	0.117 ± 0.007
150	0.098 ± 0.007	0.182 ± 0.025
200	0.068 ± 0.003	0.072 ± 0.034
250	0.070 ± 0.006	0.004 ± 0.004
350	0.201 ± 0.011	0.000 ± 0.000

Despite each test following the same engine start procedure, these figures show there to be varying peaks in concentration at various times. As the flow rate was not constant over the first 300 s of engine operation (shown in Fig. 2b), the cumulative masses for both NH_3 and N_2O are both shown in Table 3 to give a fair comparison.

The cumulative masses for NH_3 show there to be an optimum TWC temperature window to start the engine where NH_3 formation is minimised. This was between 150 ℃ and 250 ℃. The cumulative N_2O mass was found to be highest when starting the engine with the TWC between 100 ℃ and 150 ℃. Avoiding the temperature regions where NH_3 and N_2O are formed within the TWC is important due to their reported environmental effects. NH_3 emissions are undesirable due to the role of NH_3 as a secondary inorganic aerosol contributor through the formation of ammonium nitrate and ammonium sulphate which contributes to PM emissions (Huang et al. 2021). However, some studies have attempted to generate NH_3 within the TWC purposefully in order for it to later be used downstream as a reducing agent in selective catalytic reduction (SCR) systems to reduce NO_x emissions (Oh and Triplett 2014). Emissions of N_2O are also undesirable as N_2O is rated as a powerful greenhouse gas with a global warming potential 300 times that of carbon dioxide whilst also being a threat to atmospheric ozone (Hensen et al. 2013). Whilst either NH3 or N_2O are regulated under the current EURO VI emissions standard there are reports that when the EURO 7 regulations are launched these will become regulated (Mendoza-Villafuerte et al. 2017; ACEA 2020).

There are several different reaction pathways that have been proposed for the formation of NH_3 and N_2O over a TWC with typical exhaust gas inlet conditions. However, there is good agreement over the temperature ranges over which these secondary pollutants are formed. NH_3 has been reported to form over palladium-based catalysts within a temperature window between 300 ℃ and 500 ℃ (Mejía-Centeno et al. 2012; Oh and Triplett 2014; Wang et al. 2019; Liu et al. 2021a, b; Bae et al. 2022). This helps to explain the

different peaks in NH_3 concentration found in Fig. 7a. Whilst the TWC temperature is increasing, the tests with a higher TWC start temperature will transition into the NH_3 formation region sooner, hence the NH_3 peaks appear sooner after the engine start. This contrasts to the colder TWC start temperature tests where the TWC takes longer to reach the NH_3 formation region. The literature reports that N_2O formation occurs over a lower temperature region of between 150 ℃ and 300 ℃ (Jobson et al. 1994; Mejía-Centeno and Fuentes 2009; Mejía-Centeno et al. 2012; Gong and Rutland 2013). When looking at Fig. 7b, the temperatures starting at 250 ℃ and higher do not produce any N_2O. This is because these temperatures are higher than the formation region for N_2O. Therefore, the TWC does not pass through this region and no N_2O is formed. When looking at how the peak in N_2O is shifted for each different starting temperature it can be seen that the lower starting temperatures reach the formation zone later after the engine start. The inlet catalyst temperature for each start is shown in Fig. 8 with the formation regions for NH_3 and N_2O highlighted.

The formation of NH_3 and N_2O require concentrations of NO in order to form (Jobson et al. 1994; Mejía-Centeno et al. 2012; Gong and Rutland 2013; Wang et al. 2019; Bae et al. 2022). By reviewing Figs. 7 and 3b, it can be seen that the peaks in NH_3 and N_2O coincide with the NO peaks. A further strategy to reduce the chances of NH_3 and N_2O would be to manage the formation of NO within the engine. This could be achieved by maintaining the engine load at a low condition but this must be balanced against other emission, fuel economy and driveability.

Balancing unregulated emissions of ammonia and nitrous oxide

It is desirable to reduce the emissions of both NH_3 and N_2O. However, it is challenging to tackle both simultaneously since selectivity for these vary with temperature. At
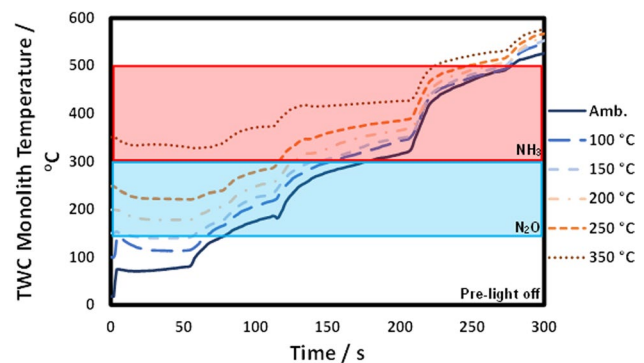

Fig. 8 TWC monolith inlet face temperature for each catalyst starting temperature. Note the highlighted temperature regions for NH_3 and N_2O formation

lower temperatures, increased selectivity towards N_2O will become an issue as highlighted by these results and other results in the available literature. Yet higher temperatures feature increased selectivity towards NH_3. The accumulated emissions for both N_2O and NH_3 in addition to the regulated emissions of CO, NO_X and HCs are shown in Fig. 9.

As discussed, CO, NO_X and HC emissions reduce as the starting temperature of the TWC is increased. It is to be highlighted in Fig. 9 that there is a large reduction in the CO and NO_X emissions from 100 to 150 ℃ which confirms the comments made in the regulated emissions section. NH_3 formation within the TWC has an optimum temperature window that appears between 150 and 250 ℃ catalyst temperature where the production is low. However, N_2O peaks for the 150 ℃ catalyst start temperature experiment. These relationships between unregulated emissions (NH_3 and N_2O) and TWC temperature change the convention that a higher TWC start temperature is always most beneficial in order to minimise emissions. In this case, the optimum starting catalyst temperature would be 250 ℃ if balancing of all emissions both regulated and unregulated is desired.

The initial temperature of the TWC varies depending upon the time between engine starts, ambient temperature, vehicle speed and catalyst insulation or heating. This will change depending upon the hybrid architecture, operating strategy and the driving style. Thus, it has to be considered
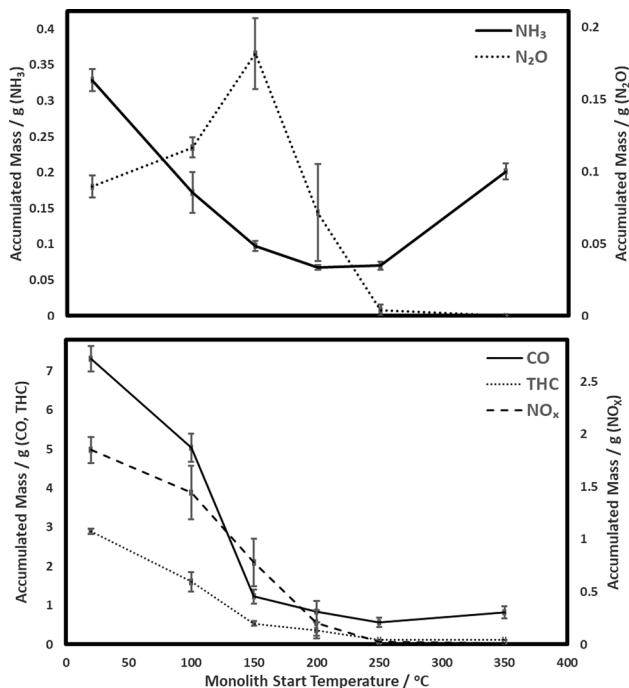
that with the reduction in temperature for a given amount of time being different for each aftertreatment set up and environment it is not possible to link accurately the starting temperatures tested here to a time between engine starts. However, despite the different EMS employed by different engineers and manufacturers it is possible to predict engine off periods. Often in the case of blended or charge-sustaining EMS, times between engine starts can be between 1 and 5 min (Overington and Rajakaruna 2015; García et al. 2019; Wang et al. 2022). This would push the engine to starting with higher TWC temperatures where NH_3 production within the TWC would be a concern. However, charge-depleting strategies feature longer engine off periods where lower TWC temperatures will be a concern (Graver et al. 2011; Wang et al. 2022). It was decided that by targeting certain catalyst temperatures rather than engine off times that this work would be applicable to PHEVs regardless of their EMS. Since it is more likely based upon the available literature that HEVs would deal with increased N_2O and NH_3 emission during each engine start, strategies should be defined to minimise these. This could involve a longer idling period to effectively limit the pre-catalyst concentration of NO_X and therefore eliminate the precursor species for N_2O and NH_3 formation. An alternative option could be to increase the engine load quickly to pass through the temperature zones with high N_2O and NH_3 production to limit the total emission per engine start. However, this may incur a fuel consumption or other regulated emission penalty.

Conclusion

This investigation has shown how regulated (CO, NO_X and HC) and unregulated emissions (NH_3 and N_2O) are affected by engine restarts over a range of catalyst temperatures that are typical of HEV operation for this particular engine and aftertreatment system setup. Regulated emissions all reduced as the catalyst temperature was increased with no emissions slip post-TWC after starting at 250 ℃ TWC temperature. This is a significant finding to provide guidelines for the selection of energy and emissions optimisation management strategies for HEVs since it suggests that by keeping the TWC above a threshold temperature at each engine start, the regulated emissions can be completely abated.

This work has also demonstrated the emissions performance for unregulated emissions. NH_3 and N_2O are expected to become regulated when the next emission regulations are released which makes these results significant for the future. NH_3 and N_2O both require NO emissions pre-TWC to be catalytically formed in the TWC. However, the formation of N_2O and NH_3 is dominant over different temperature ranges. NH_3 formation peaks at 350 ℃ whilst N_2O emission peaks at 150 ℃. To minimise both ammonia

Fig. 9 Accumulated mass of emissions for the first 500 s of engine operation with respect to the TWC temperature at the time of engine start for NH_3, N_2O, CO, NO_X and THC. Confidence intervals show the 95% confidence level calculated from 3 repeats of the start-up test

and N$_2$O emissions, a compromise must be struck between them if TWC temperature is to be optimised for each engine start.

The aim of this study was to identify how the TWC operates within a HEV with respect to the catalyst starting temperature for both regulated and unregulated emissions. This was selected as an aim due to the increased number of hybrid powertrains available on the market and the mid-term direction of the automotive industry. This work has found consensus with current literature over the formation of N$_2$O and NH$_3$ over the TWC but taken this further by linking this issue to modern HEV powertrains. This work also has provided a new direction for the optimisation of HEV energy management strategies to consider emissions of NH$_3$ and N$_2$O.

The principal limitation of this study is that it was completed using an engine dynamometer and not actual hybrid electric vehicles. This provided additional control, repeatability and instrumentation but at the expense of not using the engine as part of an actual HEV powertrain. The assumptions made on the operation were supported by the available literature, and a range of catalyst starting temperatures were selected to cover a variety of different scenarios that could be witnessed by the TWC over the journey of a HEV.

The next steps would be confirming these findings with a study operating a full hybrid electric vehicle over a driving cycle or/and in real driving emission conditions in order to evaluate the N$_2$O and NH$_3$ emissions. Further implications for this work include the evaluation of different engines and aftertreatment setups, various engine starting strategies in order to minimise the emissions of N$_2$O and NH$_3$ or targeting these emissions using a control strategy to eliminate or at least minimise the formation of these species.

Author's contributions GB conducted the investigation process, performed the experimental work and was the lead author in writing the manuscript. JMH was responsible for the manuscript ideas, formulation and the goals of the research. SZR assisted in conducting the experimental process. OD assisted in conducting the experimental process. AT was responsible for the acquisition of the financial support and providing the testing facilities to conduct the experimental work. AK provided industrial expertise to assist with the direction of the research. PM provided industrial expertise to assist with the direction of the research. All authors have contributed to the data analyses and interpretation and the review of the manuscript.

Declarations

Conflict of interest The authors declared that there is no conflict of interest.

References

ACEA. (2020). ACEA position paper views on proposals for Euro 7 emission standard.

Adhikari S, Fernando S (2006) Hydrogen membrane separation techniques. Ind Eng Chem Res 45(3):875–881

Anderson JO, Thundiyil JG, Stolbach A (2012) Clearing the air: a review of the effects of particulate matter air pollution on human health. J Med Toxicol 8(2):166–175

Anetor L, Odetunde C, Osakue EE (2014) Computational analysis of the extended zeldovich mechanism. Arab J Sci Eng 39(11):8287–8305

Awad OI, Ma X, Kamil M, Ali OM, Zhang Z, Shuai S (2020) Particulate emissions from gasoline direct injection engines: a review of how current emission regulations are being met by automobile manufacturers. Sci Total Environ 718:137302

Badshah H, Khalek IA (2015) Solid particle emissions from vehicle exhaust during engine start-up. SAE Int J Eng 8(4):1492–1502

Bae WB, Kim DY, Byun SW, Hazlett M, Yoon DY, Jung C, Kim CH, Kang SB (2022) Emission of NH$_3$ and N$_2$O during NO reduction over commercial aged three-way catalyst (TWC): Role of individual reductants in simulated exhausts. Chem Eng J Adv 9:100222

Bagheri S, Huang Y, Walker PD, Zhou JL, Surawski NC (2021) Strategies for improving the emission performance of hybrid electric vehicles. Sci Total Environ 771:144901

Bai S, Wang C, Li D, Wang G, Li G (2018) Influence of the idle-up strategy on the thermal management of diesel particulate filter regeneration during a drop to the idle process. Appl Therm Eng 141:976–980

Balas M, Lisy M, Kubicek J, Pospisil J (2014) Syngas cleaning by wet scrubber. WSEAS Trans Heat and Mass Transf 9(1):195–204

Behrentz E, Ling R, Rieger P, Winer AM (2004) Measurements of nitrous oxide emissions from light-duty motor vehicles: A pilot study. Atmos Environ 38(26):4291–4303

Bielaczyc P, Szczotka A, Woodburn J (2011) The effect of a low ambient temperature on the cold-start emissions and fuel consumption of passenger cars. Proc Inst Mech Eng Part D: J Autom Eng 225(9):1253–1264

Clarotte M, Suarez-Bertoa R, Zardini AA, Giechaskiel B, Pavlovic J, Valverde V, Astorga C (2020) Exhaust emission factors of greenhouse gases (GHGs) from European road vehicles. Environ Sci Europe, 32(125)

Farren NJ, Davison J, Rose RA, Wagner RL, Carslaw DC (2020) Underestimated ammonia emissions from road vehicles. Environ Sci Technol 54(24):15689–15697

Fernández-García M, Iglesias-Juez A, Martínez-Arias A, Hungría AB, Anderson JA, Conesa JC, Soria J (2004) Role of the state of the metal component on the light-off performance of Pd-based three-way catalysts. J Catal 221(2):594–600

García A, Monsalve-Serrano J, Sari R, Dimitrakopoulos N, Tunér M, Tunestål P (2019) Performance and emissions of a series hybrid vehicle powered by a gasoline partially premixed combustion engine. Appl Therm Eng 150:564–575

Gezer O, Kale S, Ko H, Karago Y, Pusat S, Yu L (2021) Numerical and experimental investigation of fuel consumption and CO_2 emission performance for a parallel hybrid vehicle. Alex Eng J 60:3649–3667

Gong J, Rutland C (2013) Three way catalyst modelling with ammonia and nitrous oxide kinetics for a lean burn spark ignition direct injection (SIDI) gasoline engine. SAE Technical Paper 2013–01–1572

Graver BM, Frey HC, Choi HW (2011) In-use measurement of activity, energy use, and emissions of a plug-in hybrid electric vehicle. Environ Sci Technol 45(20):9044–9051

Guille des Buttes A, Jeanneret B, Kéromnès A, Le Moyne L, Pélissier S, (2020) Energy management strategy to reduce pollutant emissions during the catalyst light-off of parallel hybrid vehicles. Appl Energy 266:114866

Heeb NV, Forss AM, Brühlmann S, Lüscher R, Saxer CJ, Hug P (2006) Three-way catalyst-induced formation of ammonia-velocity- and acceleration-dependent emission factors. Atmos Environ 40(31):5986–5997

Hensen A, Skiba U, Famulari D (2013) Low cost and state of the art methods to measure nitrous oxide emissions. Environ Res Lett 8 (025022)

Hu T, Wei Y, Liu S, Zhou L (2007) Improvement of spark-ignition (SI) engine combustion and emission during cold start, fueled with methanol/gasoline blends. Energy Fuels 21(1):171–175

Huang X, Zhang J, Zhang W, Tang G, Wang Y (2021) Atmospheric ammonia and its effect on PM2.5 pollution in urban Chengdu, Sichuan Basin, China. Environmental Pollution 291 (118195)

International Council on Clean Transportation (2019) CO_2 Emission Standards for Passenger Cars and Light-Commercial Vehicles in the European Union.

Jobson E, Smedler G, Malmberg P, Bernler H, Hjortsberg O, Gottberg I, Rosén Å (1994) Nitrous oxide formation over three-way catalyst. SAE transactions section "conclusions": J Fuels Lubric 103:519–530.

Li Y, Liu D (2011) Study on the HC emissions during cold-start conditions of gasoline direct injection engine. In: Proceedings - 4th international conference on intelligent computation technology and automation, pp 1210–1213

Liu Y, Ge Y, Tan J, Wang H, Ding Y (2021a) Research on ammonia emissions characteristics from light-duty gasoline vehicles. J Environ Sci (china) 106:182–193

Liu Y, Wang H, Li N, Tan J, Chen D (2021b) Research on ammonia emissions from three-way catalytic converters based on small sample test and vehicle test. Sci Total Environ 795:148926

Mejía-Centeno I, Castillo S, Fuentes GA (2012) Enhanced emissions of NH_3, N_2O and H_2 from a Pd-only TWC and supported Pd model catalysts: Light-off and sulfur level studies. Appl Catal B 119–120:234–240

Mejía-Centeno I, Fuentes GA (2009) Nitrous oxide formation during light-off over a commercial pd-containing three-way catalytic converter: The effect of low-sulfur gasoline. Chem Eng Commun 196(10):1140–1151

Mendoza-Villafuerte P, Suarez-Bertoa R, Giechaskiel B, Riccobono F, Bulgheroni C, Astorga C, Perujo A (2017) NOx, NH_3, N_2O and PN real driving emissions from a Euro VI heavy-duty vehicle. Impact of regulatory on-road test conditions on emissions. Sci Total Environ 609:546–555

Nevalainen P, Kinnunen NM, Kirveslahti A, Kallinen K, Maunula T, Keenan M, Suvanto M (2018) Formation of NH_3 and N_2O in a modern natural gas three-way catalyst designed for heavy-duty vehicles: the effects of simulated exhaust gas composition and ageing. Appl Catal A 552:30–37

Oh SH, Triplett T (2014) Reaction pathways and mechanism for ammonia formation and removal over palladium-based three-way catalysts: multiple roles of CO. Catal Today 231:22–32

Orecchini F, Santiangeli A, Zuccari F, Ortenzi F, Genovese A, Spazzafumo G, Nardone L (2018) Energy consumption of a last generation full hybrid vehicle compared with a conventional vehicle in real drive conditions. Energy Procedia 148:289–296

Overington S, Rajakaruna S (2015) High-efficiency control of internal combustion engines in blended charge depletion/charge sustenance strategies for plug-in hybrid electric vehicles. IEEE Trans Veh Technol 64(1):48–61

Rood S, Eslava S, Manigrasso A, Bannister C (2020) Recent advances in gasoline three-way catalyst formulation: a review. Proc Inst Mech Eng Part D J Autom Eng 234(4):936–949

Suarez-Bertoa AC (2016) Unregulated emissions from light-duty hybrid electric vehicles. Atmos Environ 136:134–143

Suarez-Bertoa R, Zardini AA, Astorga C (2014) Ammonia exhaust emissions from spark ignition vehicles over the New European driving cycle. Atmos Environ 97:43–53

The Society of Motor Manufacturers and Traders (2019) 2019 UK Automotive Sustainability Report.

Wang C, Tan J, Harle G, Gong H, Xia W, Zheng T, Zhao Y (2019) Ammonia Formation over Pd/Rh Three-Way Catalysts during Lean-to-Rich Fluctuations: The Effect of the Catalyst Aging, Exhaust Temperature, Lambda, and Duration in Rich Conditions. Environ Sci Technol 53(21):12621–12628

Wang Y, Wen Y, Zhu Q, Luo J, Yang Z, Su S, Ge Y (2022) Real driving energy consumption and CO_2 & pollutant emission characteristics of a parallel plug-in hybrid electric vehicle under different propulsion modes. Energy 244:123076

Zeng Y, Cai Y, Chu C, Kou G, Gao W (2018) Integrated energy and catalyst thermal management for plug-in hybrid electric vehicles. Energies 11:1761

Zhao C, Zu B, Xu Y, Wang Z, Zhou J, Liu L (2020) Design and analysis of an engine-start control strategy for a single-shaft parallel hybrid electric vehicle. Energy 202:117621